JETIR.ORG ISSN: 2349-5162 | ESTD Year : 2014 | Monthly Issue

JOURNAL OF EMERGING TECHNOLOGIES AND INNOVATIVE RESEARCH (JETIR)

An International Scholarly Open Access, Peer-reviewed, Refereed Journal

Discernment of intramural flaws CFRP strengthened steel structures using eddy current pulsed Thermography

Prof. Amey R. Khedikar[1], Ms. Viplavi Dongare[2]

[1]Project Guide, Department of Structural Engineering , Tulshiram Gayakwad Patil college of Engineering and Technology,Nagpur

[2]Research scholer, Department of Structural Engineering , Tulshiram Gayakwad Patil college of Engineering and Technology, Nagpur

***Abstract*:**

This study investigates the effectiveness of eddy current pulsed thermography (ECPT) to detect internal defects in CFRP reinforced metal structures. Various internal common defects of CFRP reinforced steel structures are involved in this study, which include fragmentation, low impact impact on CFRP, metal cracking, and debonding on the CFRP / steel interface. Theoretically we have analyzed the impact of these problems on the magnetic and thermal reaction of structures. To confirm the results of the theater, statistical and diagnostic tests are performed on CFRP reinforced steel plates with various types of defects. Numerical and diagnostic results indicate that the observed malformations can be assessed by ECPT and shown as regions with low temperatures in ECPT thermograms. In addition to the thermal characteristics of thermograms, the emergence of the temperature profile and temperature changes are investigated in order to further analyze the thermal response in the CFRP environment. In addition, the effectiveness of ECPT in restoring the shape and size of errors is demonstrated based on the results of the tests. In general, theoretical, numerical and experimental results show that ECPT is effective in diagnosing internal defects in CFRP reinforced steel structures, indicating that ECPT provides a promising approach to such a complex complex structure.

IndexTerms--Errors Non-destructive inspection, thermal analysis CFRP strengthens metal structures, composites, structures, faults, damage, detection and inspection, structural health monitoring etc.

I. INTRODUCTION

Incorporating Carbon fiber reinforced polymer (CFRP) into building structures has been increasingly used to restore or repair engineering steel structures such as building structures, bridges, pipelines, coastal units, vehicle and crane grid. Compared with the traditional welding method, reinforcing steel structures by binding to CFRP is more suitable in hot or explosive environments because there is no hot work involved in this process. In addition, CFRP reinforced steel structures have better resistance to corrosion and a little more weight than welded structures. At the same time, CFRP strengthens the steel structure and introduces excellent performance of strength, durability and resistance to fatigue. However, during a retrieval or subsequent service process, various defects may result in CFRP / composite structures, including subcutaneous cracks, split between CFRP layers, impact damage on CFRP, and demolition of the CFRP interface. / metal, etc. These problems diminish the functionality of the structure and present risks to the service system. These defects often produce within buildings and cannot be detected directly. Therefore, non-destructive inspection techniques (NDT) are critical to ensure the safety of CFRP reinforced steel structures. Several NDT techniques have been used in recent years to test CFRP reinforced steel structures. Acoustic emission (AE) was hired to investigate CFRP-steel bonded plate failures under rigorous laboratory testing and CFRP-steel bonded rods under tension-tension fatigue test, respectively Results show that AE is effective for phase detection of failures. and determining the methods of failure. However, AE only works for mutation errors and cannot be used to test static damage, which is very common in engineering. Piezoelectric sensors were also used to monitor CFRP metal beams by deboning. The results show that the actual proportion of impedance decreases as deboning increases. In this method, the piezoelectric sensors should be tightly connected to the tested beam and can only check the local area limited. Ultrasonic testing based on indirect lamb wave was confirmed to be effective in detecting fatigue cracks in CFRP-steel bonded plates. The lack of linearity caused by fatigue cracking was seen in representing the frequency of recovery data. However, specimens were tested and presented inconsistencies in the acquisition data. As a result, complex signal processing is required to detect cracks in fatigue. The antenna sensors were used to check for cracks in the metal substrates of CFRP-steel bonded plates. The results show that cracks can be detected by analyzing the acquisition signals using a vector network analyzer. However, the antenna sensors should be bonded to

the CFRP area using epoxy resin adhesive. At that point, the unstable antenna member may make a loud noise.

Therefore, a precisely controlled welding process or wireless test is required. Optical pulsed thermography (OPT) has also been investigated to examine the connection of CFRP-steel bonded plates. The results show that OPT is effective in detecting this type of feature. However, uneven distribution of light may cause invisible connections to the obtained thermograms. It should be concluded that there is still time

the need to develop NDT methods for CFRP reinforced steel structures. As an effective infrared thermography technique, eddy current pulsed thermography (ECPT) is effective in assessing a single driving factor. There are several documents in the ECPT for the diagnosis of a single functional disability. In particular the ECPT for steel structures, acquisition methods, data processing and retrieval of inaccurate information has been fully explored. ECPT has also been proven to be effective in CFRP, with effective input, flexibility and thermal conductivity.

However, research on ECPT for CFRP reinforced steel structures is still very limited. The only ECPT split in the steel parts of the reinforced steel structures of the CFRP has been previously investigated. Compared to single metal or single CFRP, the reinforced steel structure of CFRP exhibits different electrical and thermophysical properties. Consistently, this type of structure will produce different electromagnetic and thermal responses during ECPT. Therefore, this study aims to confirm ECPT's ability to test CFRP reinforced steel structures by investigating the thermal responses of such a composite structure during ECPT testing.

II. Literature Survey

A. Taram et. al. 2016, In this eddy current temperature study, electromagnetic induction is used to induce heat flow in objects and record its temperature response using an infrared camera. Flaw detection is based on changes in heat distribution. It is an efficient and accurate means of detecting an implicit element in metallic objects and can be grown as pulse or amplitude modulated. This paper describes simulation operations using pulsed eddy current thermometers to detect defects and measure metal objects in transmission mode. Flux2D finite element software was used.

Xin Li et. Al. 2008, In this study, Limitation of non-corrosive methods in testing carbon fiber reinforced plastic (CFRP) compounds is a major issue in the practical application of the material, especially in the aviation industry. This paper presents a study aimed at the non-destructive expressions of CFRP using current vortex methods. The relationship between the signal of different types of induction probes and the microstructure of the CFRP samples was observed. Quantitative electrical activity measurement of an object based on the analytical solution of Deeds and Dodd, providing the basis for prediction and detection of defects in fibers and properties. Optical fiber orientation specifications have also been performed on omnidirectional and indirect CFRPs using highly focused investigations. Finally, a 3D finite element (FEM) computer simulation was performed to demonstrate the integration of the probes with the sample and support the experimental method. Chapter

Chuck Hellier and. al. 2009, In this paper, the fabrication of aluminum/carbon fiber reinforced plastic (CFRP) hybrid plate using eddy current sensor in many cases is presented in this paper. Circular air sensors and sensors with high ferritic core sensors are designed for bulk conductivity measurement and directional characterization. An analytical model describing the interaction of a circular sensor with a hybrid planar structure is developed. Finite element (FE) models that take into account the CFRP anisotropy are also proposed. Both models are in good agreement with the test results. The characteristics of sensory signals are analyzed and interpreted. This is believed to be the first published report on the use of current eddy current techniques in the production of aluminum/CFRP hybrid materials..

Literature Summary

By studying various materials and methods, it has been confirmed that the Eddy Current Pulse Thermometer (ECPT) is one of the new diagnostic and test methods (NDT&E) has been used to check rail integrity, especially in communication fatigue (RCF) detection and crack sizing. This paper proposes a framework for exploratory analysis (POD) for ECPT system. In particular, three distinct features, namely high temperature response, first-order variance prediction, and first-order dissociated image map, are used to measure angular slit length by inserting a line. Based on the positive relationship between these factors and the clearance length, the POD curves of the ECPT system based on the coil line for angular strain detection were calculated and compared. The results show that the high temperature responsive element has high frequency and visibility obtained in a short space. Unique superlative image and rating board features are appealing to capture long spaces.

III. Methodology

3.1. Fundamental of ECPT

The ECPT method combines current eddy testing with infrared thermography. During ECPT, coils with other waves form another magnetic field. Then, the disputed magnetic field results in eddy currents in the test area. Attractive editing currents only propagate to the fixed depths of the object. Skin depth is used to describe the depth at which the current in conductor decreases to 1 / e of the current local pressure. Skin depth is calculated as follows:

$$\delta = \frac{1}{\sqrt{\pi f \mu \sigma}} \quad (1)$$

where when d is the depth of the skin, f the frequency of the excitement current, l and r the magnetic field and the electrical current of the object, respectively. According to Eq.1, the skin depth of CFRP and that of the metal is approximately 50 mmand 30lm lm, respectively. The density of eddy currents formed is related to the electromagnetic properties of the material.

The permeability of CFRP is much lower than that of metal materials. As a result, eddy currents frozen in CFRP are much weaker and less noticeable compared to those in the metal part. In experimental materials, eddy currents attracted produce Joule heat, which is the source of internal heat for infrared thermography testing. The relationship between Joule heat and eddy currents is defined as:

$$Q = \frac{1}{\sigma}|J_S|^2 = \frac{1}{\sigma}|\sigma E|^2 \quad (2)$$

where JS is the eddy current density, E is the electric field pressure and Q is the Joule temperature generated by the eddy currents. As an internal heat source, the Joule temperature causes the temperature to rise in the

corresponding areas of the object being tested. Due to the uneven distribution of eddy currents in an object, the amplitude of the rising temperature varies accordingly to the object. This temperature gradient results in the magnification of the temperature from the highest temperature to the lowest temperature of one object.

The presence of a defect in the tested object may affect the current eddy distribution and interfere with subsequent heat conduction. These effects caused by disability can lead to abnormal temperatures in the problem areas in the area. By recording the distribution of temperature in an object using a hot image, the corresponding regions can be detected by thermograms obtained because of their unusual temperatures.

3.2. ECPT for defects detection in CFRP strengthened steel structures

3.2.1. Common ECPT Method for Detection of CFRP Reinforced Steel Structures Based on the ECPT framework, Figure 1 describes the ECPT standard diagnostic method for detecting defects in the CFRP reinforced steel structure. As shown in Fig. 1, eddy current is applied to the metal part and CFRP by high-frequency current fluctuations in the coil. As previously analyzed, eddy currents in CFRP are very weak and overlooked. Therefore a small amount of Joule heat is produced in CFRP. At the same time, the corresponding temperature of the current eddy Joule causes a significant increase in temperature in the metal part. The gradient of temperature between the metal part and the CFRP results in a continuous increase in temperature and an additional temperature rise in the CFRP. This thermal conduction ceases until the thermal balance is finally reached within the entire reinforced steel structure of the CFRP.

In the case of a disability detection, the presence of defects in the CFRP reinforced steel structures, including fragmentation between CFRP layers, low-speed damage to the CFRP, cracking of the metal substrate, and demolition of the CFRP / steel interface, will affect the production process heat and heat transfer in different ways..

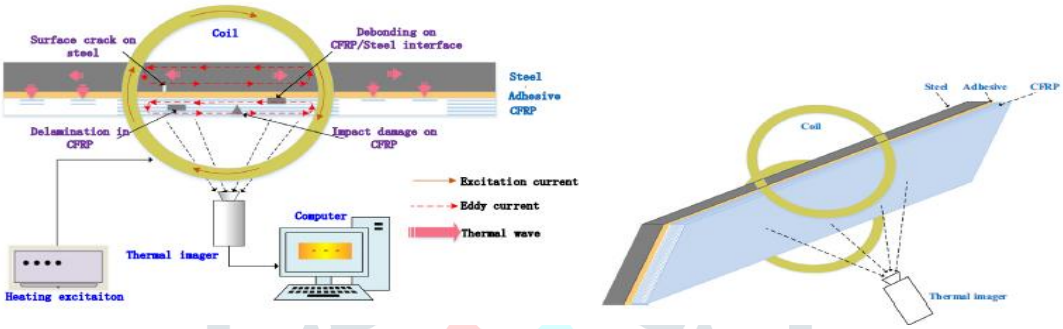

Fig. 2. Schematic of the proposed method for defects detection in CFRP

Such influences thus result in the abnormal temperature distribution in the CFRP area. This confusing temperature distribution can be recorded by a hot photo shooter. The presence of defects can be detected in the received thermograms and the characteristics of the defect can be restored with a specific temperature pattern recorded in the thermograms.

3.2.2. ECPT detection methods for debonding, delamination and low-impact effects on CFRP reinforced steel structures Figure 2 shows the electrical and thermal response of CFRP steel. Bound structure with delamination, debonding and low impact effects during ECPT testing. Figure 2 (a) also shows the coil arrangement and test element, corresponding to the test setup shown in the next section.

As shown in Fig. 2 (a), debonding creates a connection between the CFRP and the metal component, while a split occurs between two adjacent layers of the CFRP. Both are airborne joint defects and may occur in the reset process due to insufficient adhesion or insufficient pressure. The impact of low speed often leads to internal damage that can be detected by visual inspection. These internal damage may be cracks in the matrix, cracks in the adhesive, debondings or delaminations.

These problems can severely damage the structure of the structure. Figure 2 (a) shows the coil-stirring waves and eded currents in the tested CFRP certified metal sample. As shown in Fig. 2 (a), eddy currents attracted to the metal part spread to shallow depths below the surface due to the skin effect.

Additionally, due to the weak electromagnetic properties of CFRP, the eddy currents produced in CFRP are very weak and overlooked. Because debonding, delamination and impact damage are found outside the metal part, there is little impact on the current distribution of eddy on the metal part, as shown in Fig. 2 (a). Figure 2 (b) shows the heat of the Joule produced by the eddy currents in the CFRP reinforced steel structure during heating. stage. Due to the eddy current skin effect, the corresponding heat of the Joule also concentrates on the metal binding. At the same time, a small amount of Joule heat produces in CFRP due to negligible eddy currents. As a result, there is a temperature difference between the metal part and the CFRP. Due to this temperature gradient, the heat of the Joule on the metal part leads to CFRP near the thickness direction, as indicated by the red arrows in Fig. 2 (b). Figure 2 (c) shows the hot response instead of CFRP ina time when sufficient Joule heat has been carried from the metal part to the CFRP area. Compared to surrounding adhesive material, debonding and delamination have lower thermal conductivity as air permeability. During the thermal conductivity process, these two types of factor affect the thermal reaction of the structure as heat dissipation barriers. Therefore, the corresponding.

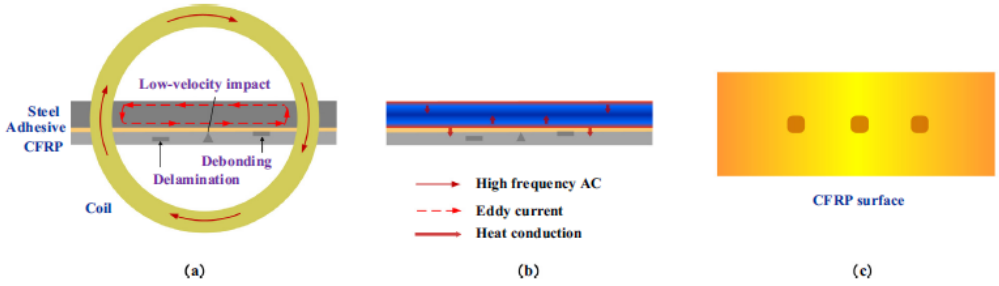

Fig. 2. Electromagnetic and thermal response of a CFRP-steel bonded structure with a delamination, a debonding and a low velocity impact damage: (a) the electromagnetic
response (b) the thermal response during the heating stage (c) the thermal response after heating.

Debonding and delamination regions in the CFRP area receive less heat compared to other regions. As a result, these contiguous convex areas bring low temperatures, as shown in Fig. 2 (c). Like debonding and delamination, internal damage caused by the impact of low speed can also prevent heat transfer from steel to CFRP. Therefore, the corresponding circuit of the impact of the low-speed impact also showed a low temperature response, as shown in Fig. 2 (c).

2.2.3. ECPT detection methods for surface cracking of CFRP reinforced steel structures CromRP electromagnetic and thermal reaction of CFRP reinforced steel structure with excess cracking in the metal part are shown in Fig. 3. Figure 3 (a) shows the effect of the cracks in the current eddy spread of the metal binding area. Figure 3 (b) shows the hot response in the metal binding area. The heat reaction in the CFRP area is shown in Fig. 3 (c). Figure 3 shows that in contrast to debondings or delaminations, cracks in the metal binding area greatly affect the current distribution of eddy. As mentioned earlier, eddy currents focus on shallow depths on the metal part. As a result, eddy currents are prevented from cracking and should pass down or split tips. Therefore, the current eddy density becomes larger at the edges of the cracks and at the lower part of the cracks. The corresponding temperature of the Joule is concentrated in these regions. In addition, cracking also disrupts the subsequent thermal conductivity within the metal part. This causes heat to accumulate on both sides of the crack. In short, the higher temperatures on the tips, sides and bottom of the crack than crack, leading to a lower cracking temperature. This feature of low crack temperatures in the metal binding transmits to the CFRP area due to the temperature associated with the solid surface. Finally, the fractured region in the CFRP area shows lower temperatures than the surrounding regions. This low temperature crack feature can be recorded hot photo and displayed on the received thermograms.

IV. Numerical Analysis

3.1. Numerical analysis of ECPT detection for CFRP strengthened steel structure with debonding and delamination :

Numerical analysis was performed using the AC / DC module and the heat transfer module in the COMSOL5.2a Multiphysics software. Electromagnetic-thermal 3-D models of CFRP reinforced metal plates with debonding or delamination are formed as shown in Figure 4. The dimensions of CFRP and steel in the model are set as 110 mm _ 30 mm _ 1 mm and 110 mm _ 30 mm _ 6 mm, respectively. Steel plates have the same thickness and length in numerical modeling and testing. The length of the steel plate is reduced to 110 mm to reduce the calculation load on the value scale under the basis that the length of the steel plate is greater than the width of the coil. At the same time, the joints and divisions of 8 mm _8mm_ 0.2 mm are built into the CFRP / metal interface and CFRP, respectively.

Part of the metal and coils were made with a mechanical map while part of the CFRP was combined with free tetrahedral material. The size of the element in defective regions was controlled within 0.1 mm and in some regions it was limited to 1 mm (Fig. 5). The properties of the materials used in this work are shown in Table 1. The coupling and delamination are filled with air and the coil is supplied with copper material. According to experiments, the initial temperature was set as 293 K. The excitation current of 200A and 195 kHz is used to produce the magnetic flux of the input temperature.

The heating time is 700 ms, followed by the cooling stage of 19000 ms to detect the emergence of heat dissipation. Based on the electromagnetic-thermal 3-D material model, the ECPT testing process for CFRP reinforced steel structures by disintegration and delamination is investigated, respectively. Integration structures are presented in Figure 6, which shows the similar and satisfactory combination of the two types of disabilities.

Many of the physical interactions of electromagnetic-thermal effects are analyzed by considering the magnetic flux, eddy current and the resulting temperature throughout the model. The quantity of magnetic flux and the maximum current density are listed in Fig. 7. The arrows in Fig. 7 (a) shows the direction of the magnetic field and that in Fig. 7 (b and c) shows the direction of the currents formed. It can be noted that a nearly vertical magnetic field is produced in a structure within the range of the coil as the variable strength of the high waves passes through the coil. Figure 7 (b and c) shows that eddy currents are primarily present in the steel plate areas within the coil width. Figure 7 (d) shows that the current small eddy produces in CFRP due to its weak electromagnetic properties. Figure 7 (b and c) also shows that debonding and delamination have the same electromagnetic response. Both debonding and delamination drawings have no specific references to current eddy distribution maps. This suggests that debonding and delamination do not affect the magnetic field and current eddy distribution during ECPT.

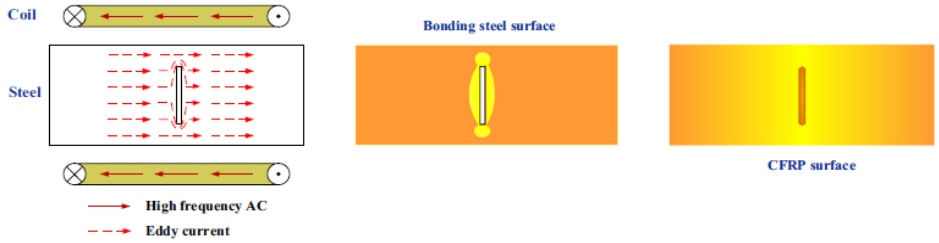

Fig. 3. Electromagnetic and thermal response of a CFRP-steel bonded structure with a crack in the steel bonding surface: (a) the electromagnetic response (b) the thermal response during the heating stage (c) the thermal response after heating.

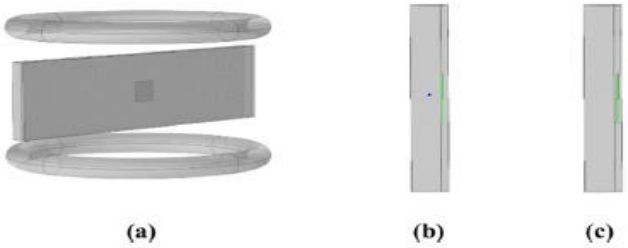

Fig. 4. Numerical model of ECPT detection for CFRP strengthened steel structures with debonding or delamination: (a) overall model (b) enlarged cross-section of debonding (c) enlarged cross-section of delamination.

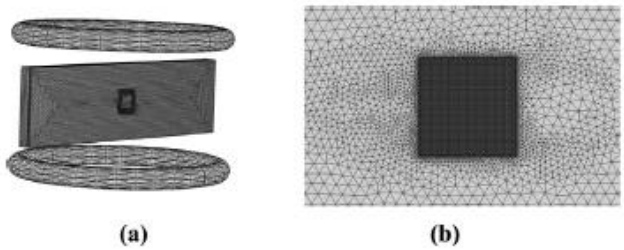

Fig. 5. Meshed model of ECPT detection for CFRP strengthened steel structure with debonding or delamination: (a) overall meshed model (b meshed debonding or delamination.

As most eddy currents produce in the metal part and eddy currents produced in CFRP are very limited, the corresponding temperature of the Joule also produces in the metal part. This causes the temperature between the metal and the CFRP. The heat will then be transferred from the metal part with the highest temperature to the lowest CFRP temperature near the tension line. Temporary temperature distribution in the CFRP area at 2.5 s is shown in Fig. 8. The corresponding clicking and delamination regions in the CFRP area show a low temperature reaction in Fig. 8, indicating that these parallel circuits receive less heat compared to others. regions. It can be assumed that debonding and delamination prevent heat transfer from the metal part to the CFRP area.

In general, it can be concluded that debonding and delamination do not affect the magnetic field and current eddy distribution but interfere with the heat transfer from the metal part to the CFRP area.

This interference from heat induction causes indications of low binding temperatures and shrinkage.

3.2. Numerical analysis of ECPT detection for CFRP strengthened steel structure with a crack

An electromagnetic-thermal 3-D detection model of ECPT for a fragmented CFRP reinforced steel structure is also developed, as shown in Figure 9. The magnitude of the CFRP and the metal in the model is the same as the magnitude described in section. 3.1.

The size of the crack found in the metal binding area is 2 mm_30 mm _ 2 mm. In addition, the initial temperature, excitation current, temperature length and cooling time correspond to the previous phase. Numerical analysis was performed using this electromagnetic-thermal 3-D model to mimic the ECPT testing process for CFRP reinforced metal structures with cracks in the metal substrate. The structure of the combination is shown in Figure 10, which shows the satisfactory combination of numerical analysis.

Table 1 : Material properties.

Materials	CFRP	Steel	Copper	Air
Electrical conductivity σ [S/m]	{10000, 100, 100}	1.12e7	5.998e7	0
Relative permeability μ	1	4000	1	1
Density ρ [kg/m^3]	1540	7870	8700	1.29
Heat capacity C_ρ [J/(kg.K)]	850	440	385	1000
Thermal conductivity k [W/(m.K)]	{2.2, 1.4, 0.6}	76.2	400	0.023

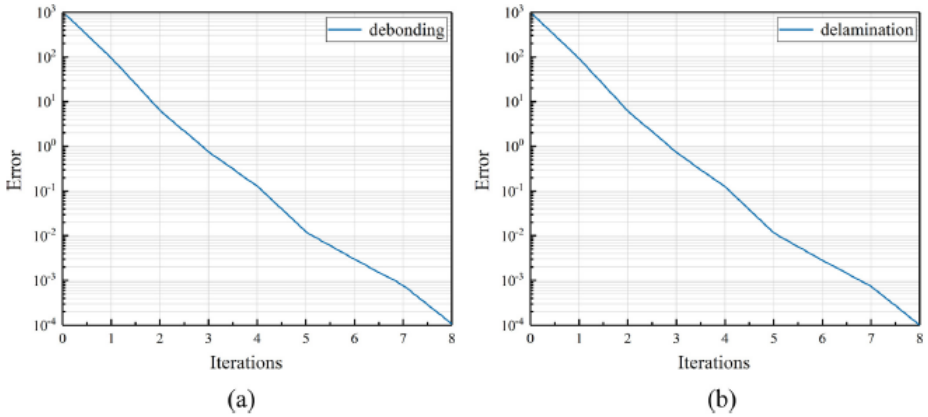

Fig. 6. Convergence plots of numerical simulation for ECPT inspection of CFRP strengthened steel structures with (a) debonding and (b) delamination.

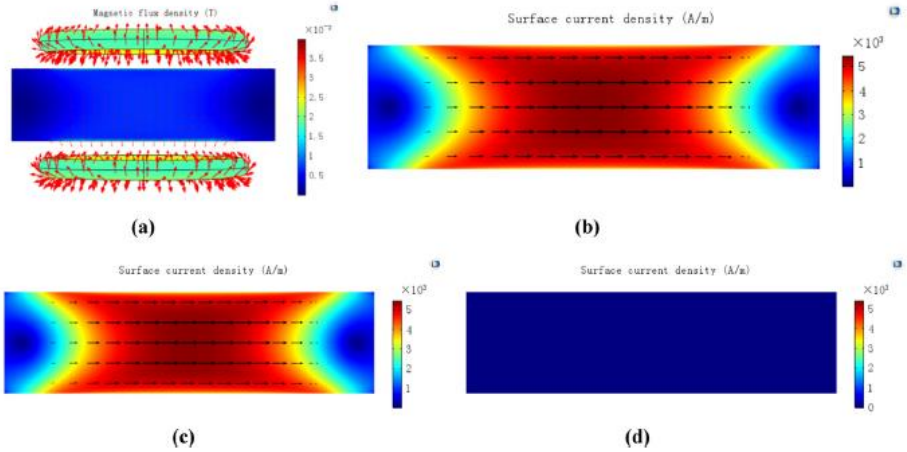

Fig. 7. Electromagnetic responses of CFRP strengthened steel structure with debonding and delamination: (a) magnetic flux density (b) steel surface current density in the case where the strengthened structure contains debonding (c) surface current density of steel in the case where the strengthened structure contains delamination (d)surface current density of CFRP.

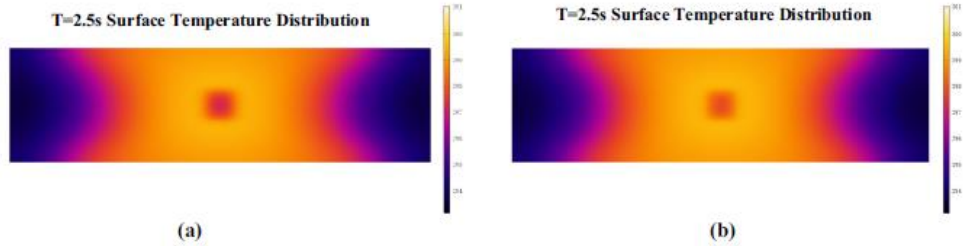

Fig. 8. The surface temperature distribution of CFRP strengthened steel structure with defects of (a) debonding (b) delamination.

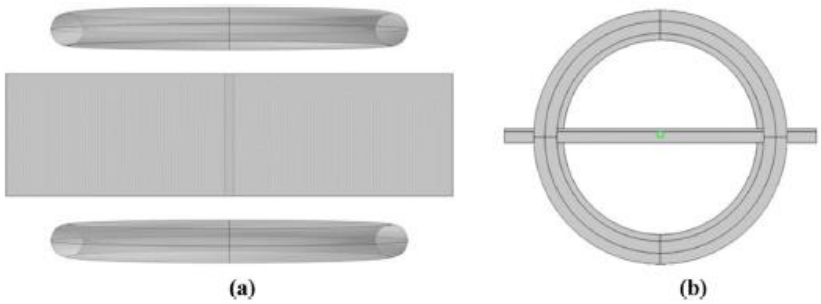

Fig. 9. The numerical model of ECPT detection for CFRP strengthened steel structure with a crack: (a) front view (b) top view.

The magnetic flux density and surface current density are listed in Fig. 11. It may be noted that in order to investigate for fractures, eddy currents are restricted and must be transferred to a lower surface. As a result, eddy current density becomes larger on the fracture sides and at the bottom, resulting in a corresponding Joule temperature concentration in these regions. The distribution of excess temperatures in the metal binding and before CFRP is shown in the figure. 12. We see that the low-temperature element is exposed to the cracked surface and high temperatures appear on the edges of the cracks. As mentioned earlier, eddy currents focus on the cracks and cracks at the bottom of the crack while there are no eddy currents producing in the airy environment. As a result of this current eddy distribution, the extra heat of the Joule produces the surrounding sides. In the air-filled crack region, there are no eddy current productions and no corresponding Joule heat gifts. Thus, the air-filled crack region and the crack side in the universe exhibit different temperature characteristics. This temperature difference in

the metal binding is transmitted to the CFRP area due to the temperature corresponding to the thickening line.

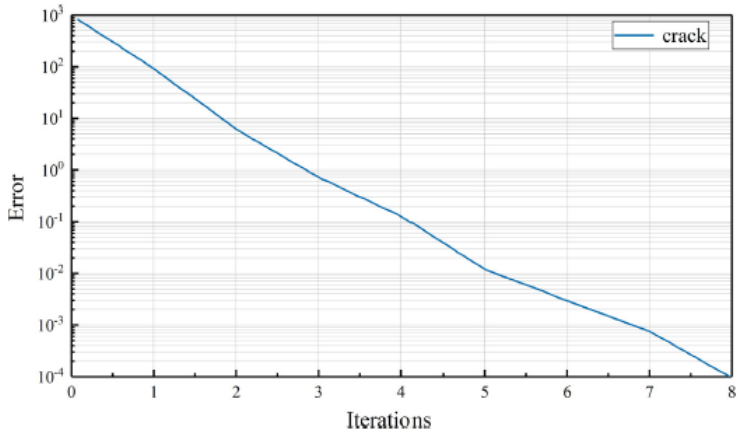

Fig. 10. Convergence plots of numerical simulation for ECPT inspection of CFRP strengthened steel structures with cracks

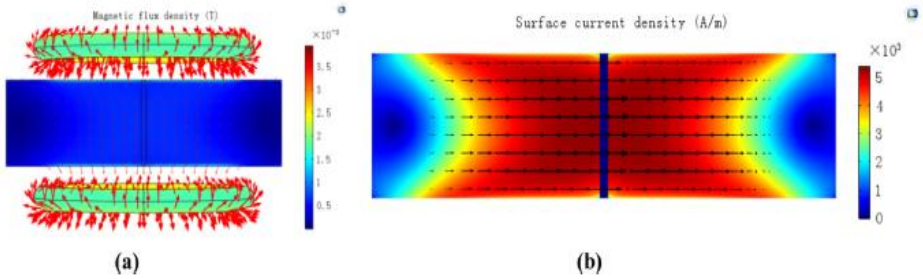

Fig. 11. Electromagnetic response of a CFRP strengthened steel structure with a crack. (a) magnetic flux density (b) surface current density.

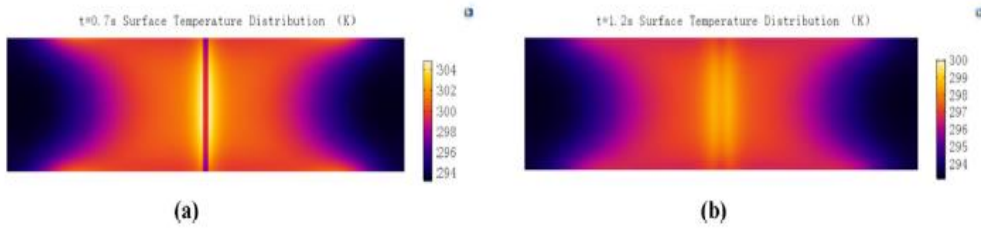

(a) (b)

Fig. 12. The temperature distributions of different surfaces of CFRP strengthened steel structure with crack: (a) steel bonding surface; (b) CFRP surface.

As a result, such specific heat-induced thermal effects can eventually be seen in the CFRP surface thermograms on Fig. Fig. 12 (b). In general, it can be concluded that cracking significantly affects the current distribution of eddy on the metal part. There is no current eddy temperature and Joule compatibility in an air-filled crack, which leads to a lower temperature factor. Then this is the low temperature feature of the fracture transfer in the CFRP area and can be recorded by a hot photographer. Finally, the crack-related region exhibits low temperature characteristics in captive thermograms.

V. Conclusion

In this study, the effectiveness of Eddy Current Pulse Temperature (ECPT) for detecting CFRP reinforced steel structures was analyzed and confirmed. Internal faults were investigated, including CFRP connection/metal interface, CFRP layer fragmentation, metal base cracking, and low-speed CFRP damage. According to the results of theoretical analysis and testing, it is concluded that ECPT successfully detects various defects in reinforced steel structures before CFR, providing a promising and accurate method to ensure service life. of this composite structure. Future work will focus on ECPT's ability to detect other types of defects in CFRP/structural steel structures and the impact factors including adhesion, CFRP layer thickness and size of systematic tests.

In this work, pulsed thermography method is used in metal structure to detect wall defects.
The basics of TSR, PPT, and PCT have been updated for thermal imaging and analysis. The effectiveness of each signal processing method was evaluated based on improved defect detection and SNR. Based on the results, it was decided
That significant improvements in feature detection and SNR values could be achieved after strategy implementation. TSR provides lower resolution images than green thermal images and offers significant improvements in defect detection through enhanced spatial and temporal tuning as well as the ability to create time images. However, variation of results in different cases or frameworks can be detrimental to TSR.

PPTs were found to be very sensitive to feature depth and provide the primary SNR for both small and deep flaws. However, the effects of PPTs are sometimes difficult to manage because they provide a lot of data for different spectra. PCT has been shown to be helpful in diagnosing problems large and small. Frame number independent results have proven to be a key advantage of PCT.

Future work will focus on using pulsed photothermal signal processing techniques to detect actual faults in pipeline structures. In addition, the maximum depth detection capability of the pulse thermometer will be investigated. In addition, analysis based on TSR will be performed with high polynomial degree. Finally, error analysis strategies will also be considered for the results obtained.

References

[1] Emmanuel P. Papadakis, “Quality degradation due to shipment of nonconforming product under statistical process control in the absence of quarantining”, Materials Evaluation, Vol. 51(11), pp. 1274–1278, 1993.
[2] P J James, “The role of non-destructive testing in the control of boiler tube failures”, Insight, Vol. 37(2), pp. 179-183, 1995.
[3] Chuck Hellier, “Handbook of Non-destructive evaluation”, McGraw-Hill Professional, 2001, ISBN0-07-028121-1; ISBN0-07-139947-X.
[4] K. N. Hitchcock, “Design evaluation through improved non-destructive testing technology”, British Journal of NDT, Vol. 33(4), pp. 167-171, 1991.
[5] P.J. Heffernan, “Fatigue behaviour of reinforced concrete beams strengthened with CFRP laminates”, PhD thesis, Royal Military College of Canada, 1997.
[6] J. Waller, “Carbon fibre cement composites”, Civil Engineering and Public Works Review 67, 789, pp. 357—361, 1972.
[7] M. P. De Goeje and K. E. D. Wapenaar, “Non-destructive inspection of carbon fibre-reinforced plastics using eddy current methods”, Composites, Vol. 23(3), pp. 147-157, 1992.
[8] Barret R, “All-moving active aerodynamic surface”, Research in Smart Materials and Structures, Vol. 4, pp. 65-71, 1995.
[9] Hanselka H, “Realization of smart structures by using fiber composite materials”, Smart Mechanical Systems-Adaptronics, pp. 1-10, Dusseldorf, 1997.
[10] A. Briggs, “Review: Carbon fibre-reinforced cement”, Journal of Materials Science, Vol. 12, pp. 384—404, 1977.
[11] McGuire, M.F. Stainless Steels for Design Engineers; ASM International: Materials Park, OH, USA, 2008.
[12] Baddoo, N. Stainless Steel in Construction: AReview of Research, Applications, Challenges and Opportunities. J. Constr. Steel Res. **2008**, 64, 1199–1206. [CrossRef]
[13] Lister, D.H.; Cook, W.G. Nuclear Plant Materials and Corrosion. Available online: https: //www.unene.ca/essentialcandu/pdf/14%20-%20Nuclear%20Plant%20Materials%20and%20Corrosion.pdf (accessed on 2 June 2020).
[14] Okada, H.; Uchida, S.; Naitoh, M.; Xiong, J.; Koshizuka, S. Evaluation Methods for Corrosion Damage of Components in Cooling Systems of Nuclear Power Plants by Coupling Analysis of Corrosion and Flow Dynamics (V) Flow-Accelerated Corrosion Under Single-and Two-Phase Flow Conditions. J. Nucl. Sci. Technol. **2011**, 48, 65–75. [CrossRef]

[15] Ahmed, W.H. Flow accelerated corrosion in nuclear power plants. In Nuclear Power-Practical Aspects; Anonymous, Ed.; IntechOpen: Rijeka, Croatia, 2012.
[16] Naitoh, M.; Okada, H.; Uchida, S.; Yugo, H.; Koshizuka, S. Evaluation Method for Pipe Wall Thinning due to
Liquid Droplet Impingement. Nucl. Eng. Des. **2013**, 264, 195–202. [CrossRef]
[17] Onel, Y.; Ewert, U.; Willems, P. Radiographic Wall Thickness Measurement of Pipes by a New Tomographic Algorithm. In Proceedings of the 15th WCNDT, Roma, Italy, 15–21 October 2000; pp. 1–6.
[18] Edalati, K.; Rastkhah, N.; Kermani, A.; Seiedi, M.; Movafeghi, A. The use of Radiography for Thickness Measurement and Corrosion Monitoring in Pipes. Int. J. Press. Vessel. Pip. **2006**, 83, 736–741. [CrossRef]
[19] Rakvin, M.; Markuˇciˇc, D.; Hižman, B. Evaluation of PipeWall Thickness Based on Contrast Measurement using Computed Radiography (CR). Procedia Eng. **2014**, 69, 1216–1224. [CrossRef]
[20] Ju, Y. Remote measurement of pipe wall thinning by microwaves. In Advanced Nondestructive Evaluation II: Volume 2; Anonymous, Ed.;World Scientific: Busan, Korea, 2008; pp. 1128–1133.
[21] Liu, L.; Ju, Y. A High-E_ciency Nondestructive Method for Remote Detection and Quantitative Evaluation of Pipe Wall Thinning using Microwaves. NDT E Int. **2011**, 44, 106–110. [CrossRef]
[22] Liu, L.; Ju, Y.; Chen, M. Optimizing the Frequency Range of Microwaves for High-Resolution Evaluation of Wall Thinning Locations in a Long-Distance Metal Pipe. NDT E Int. **2013**, 57, 52–57. [CrossRef]
[23] Nishino, H.; Takemoto, M.; Chubachi, N. Estimating the Diameter Thickness of a Pipe using the Primary Wave Velocity of a Hollow Cylindrical GuidedWave. Appl. Phys. Lett. **2004**, 85, 1077–1079. [CrossRef]
[24] Leonard, K.R.; Hinders, M.K. Lamb Wave Tomography of Pipe-Like Structures. Ultrasonics **2005**, 43, 574–583. [CrossRef]
[25] Cheong, Y.; Kim, K.; Kim, D. High-Temperature Ultrasonic Thickness Monitoring for Pipe Thinning in a Flow-Accelerated Corrosion Proof Test Facility. Nucl. Eng. Technol. **2017**, 49, 1463–1471. [CrossRef]
[26] Alobaidi, W.M.; Kintner, C.E.; Alkuam, E.A.; Sasaki, K.; Yusa, N.; Hashizume, H.; Sandgren, E. Experimental Evaluation of Novel Hybrid Microwave/Ultrasonic Technique to Locate and Characterize PipeWall Thinning. J. Press. Vessel Technol. **2018**, 140, 011501. [CrossRef] 17. Jinfeng, D.; Yihua, K.; Xinjun, W. Tubing Thread Inspection by Magnetic Flux Leakage. NDT E Int. **2006**, 39, 53–56. [CrossRef]
[27] Zhang, Y.; Yan, G. Detection of Gas Pipe Wall Thickness Based on Electromagnetic Flux Leakage. Russ. J. Nondestruct. Test. **2007**, 43, 123–132. [CrossRef].